General Disclaimer

One or more of the Following Statements may affect this Document

- This document has been reproduced from the best copy furnished by the organizational source. It is being released in the interest of making available as much information as possible.

- This document may contain data, which exceeds the sheet parameters. It was furnished in this condition by the organizational source and is the best copy available.

- This document may contain tone-on-tone or color graphs, charts and/or pictures, which have been reproduced in black and white.

- This document is paginated as submitted by the original source.

- Portions of this document are not fully legible due to the historical nature of some of the material. However, it is the best reproduction available from the original submission.

NASA

Technical Memorandum 79556

Reflection Spectra and Oxides and Natural Surfaces

Peter Wasilewski

MAY 1978

National Aeronautics and
Space Administration

Goddard Space Flight Center
Greenbelt, Maryland 20771

BIBLIOGRAPHIC DATA SHEET

1. Report No.	2. Government Accession No.	3. Recipient's Catalog No.
TM 79556		

4. Title and Subtitle	5. Report Date
Reflection Spectra and Magnetochemistry of Iron Oxides and Natural Surfaces	May 1978
	6. Performing Organization Code: 691
7. Author(s): Peter Wasilewski	8. Performing Organization Report No.
9. Performing Organization Name and Address: Goddard Space Flight Center, Greenbelt, Maryland 20771	10. Work Unit No.
	11. Contract or Grant No.
	13. Type of Report and Period Covered: Technical Memorandum
12. Sponsoring Agency Name and Address	14. Sponsoring Agency Code
15. Supplementary Notes	

16. Abstract

The magnetic properties and spectral characteristics of iron oxides are distinctive. Diagnostic features in reflectance spectra (0.5 to 2.4 μm) for αFe_2O_3, γFe_2O_3 and FeOOH include location of Fe^{3+} absorption features, intensity ratios at various wavelengths (in particular R(0.6)/R(0.75 μm), R(1.0 μm)/R(1.2 μm)), the curve shape between 1.2 μm and 2.4 μm.

The reflection spectrum of natural rock surfaces are seldom those of the bulk rock because of weathering effects. Stains provide "overprints", while coatings may obscure the bulk material entirely. Coatings are found to be dominated by iron oxides and clay. This simple macroscopic model of rock spectra (based on concepts of stains and coatings) is considered adequate for interpretation of LANDSAT data.

The magnetic properties of the materials associated with specific spectral types and systemmatic changes in both spectra and magnetic properties are considered. The magnetic properties of an asteroid can be specified by virtue of a match between laboratory meteorite spectra and telescope reflectivity spectra from asteroids. If the Martian surface contains a montmorillonite clay, the clay must be iron rich, and in a low state of hydration. Available Mars spectra is of insufficient resolution to provide an identification of species responsible for the coloration of the surface.

17. Key Words (Selected by Author(s))	18. Distribution Statement
Reflection spectra, Martian surface, Iron oxides, Rock surfaces, Magnetochemistry	

19. Security Classif. (of this report)	20. Security Classif. (of this page)	21. No. of Pages	22. Price*
U	U	44	

*For sale by the National Technical Information Service, Springfield, Virginia 22151.

GSFC 25-44 (10/77)

REFLECTION SPECTRA AND MAGNETOCHEMISTRY OF IRON OXIDES AND NATURAL SURFACES

by

Peter Wasilewski
Laboratory for Extraterrestrial Physics
NASA/Goddard Space Flight Center
Greenbelt, Maryland 20771

SUMMARY

The magnetic properties and spectral characteristics of iron oxides are distinctive. Diagnostic features in reflectance spectra (0.5 to 2.4 μm) for αFe_2O_3, γFe_2O_3 and FeOOH include location of Fe^{3+} absorption features, intensity ratios at various wavelengths (in particular R(0.6)/R(0.75 μm), R(1.0 μm)/R(1.2 μm)), the curve shape between 1.2 μm and 2.4 μm.

The reflection spectrum of natural rock surfaces are seldom those of the bulk rock because of weathering effects. Stains provide "overprints", while coatings may obscure the bulk material entirely. Coatings are found to be dominated by iron oxides and clay. This simple macroscopic model of rock spectra (based on concepts of stains and coatings) is considered adequate for interpretation of LANDSAT data.

The magnetic properties of the materials associated with specific spectral types and systematic changes in both spectra and magnetic properties are considered. The magnetic properties of asteroids can be specified by virtue of laboratory meteorite spectra matches with telescope reflectivity spectra from asteroids. If the Martian surface contains a

montmorillonite clay, the clay must be iron rich, and in a low state of hydration. Available Mars spectra is of insufficient resolution to provide an identification of species responsible for the coloration of the surface.

INTRODUCTION

A reflection spectrum represents the fraction of incident radiation reflected from the surface as a function of wavelength. Natural rock surfaces are generally admixtures of exposed rock and weathering products. Reflection spectra are further influenced by physical characteristics such as surface roughness which is in turn related to grain size and rock texture. Much of the available spectral information derives from laboratory studies of powdered rock and pure minerals (Adams & Felice, 1967; Hunt et al. (1971; 1973a; 1973b; 1973c; and many others) and is therefore of limited use in evaluation of real rock surfaces. Soil colors are also strongly dependent on the nature of weathering products and in particular of iron compounds. Such systems represent the actual surfaces viewed by LANDSAT and the Viking Landers.

Weathering products are to a large extent composed of oxides, oxyhydrates, and oxyhydroxides of varying degrees of crystallinity. Magnetic techniques can in principle be used to characterize the Fe products since each pure species has a characteristic set of magnetic properties (Wasilewski, 1974). These magnetic properties can be used to follow the alteration of the Fe species. In addition, depth of weathering can be characterized using magnetic techniques.

In this paper the magnetic properties and diagnostic reflection spectra for Fe-Fe_3O_4-γFe_2O_3, αFe_2O_3 and FeOOH are presented and several examples of natural rock surfaces, soils, clays and powdered rock are

considered. The primary aim of this paper is to identify the diagnostic features of Fe oxide spectra and establish the connection between magnetic properties and the reflection spectra.

SPECTRAL MEASUREMENTS

Reflection spectra (0.5 μm to 1.2 μm) of Fe, Fe_3O_4, γFe_2O_3, αFe_2O_3 and FeOOH have been found to be distinctive (Wasilewski, 1974). Data of Liese (1969) and Kodama et al., (1977), extend the iron oxide "fingerprints" out to 33 μm. These results suggest that the spectral range between 0.5 μm and 33 μm can be used to characterize in some detail the relative significance of iron oxides and clays in natural weathered surfaces since clays and iron oxides are easily discriminated. Reflectance curves were measured in conventional manner on a dual beam CARY 14 recording spectrophotometer, with a smoked $BaSO_4$ reference.

BRUDERHEIM CHONDRITE (L6)

Reflectance spectra for mineral separates from the Bruderheim (L6) chondrite are shown in Figure 1a. Magnetic hysteresis loops (measured at 78K) for each of the separates are shown in Figure 2 - the values of paramagnetic susceptibility and the saturation moment of the ferromagnetic impurity are indicated. Also included in Figure 1a is the reflectance spectrum for Fisher electrolytic iron powder. The silicates have the appropriate absorption features (Adams, 1974) while metal and troilite are featureless, the reflectance increasing with wavelength as expected (see Gaffey, 1975), and are therefore different from Fe_3O_4 which has a flat reflection spectrum with a broad and shallow absorption centered near 1.0 μm.

OXIDATION OF Fe_3O_4 AND THERMAL DECOMPOSITION OF $\alpha FeOOH$ and γFe_2O_3

Changes in reflectance associated with oxidation of Fe_3O_4 powder (1 μm - 7029) are documented in Figure 1B. The experiment consisted of heating one each of 6 identical dishes of 7029 in an open ended tubular furnace at each of the indicated temperatures for one hour. Samples were X-rayed using a Norelco diffractometer with iron filtered Co radiation (Figure 3). Fe_3O_4 (A) had an I_S (saturation magnetization) value of 94 emu/gm, the γ phase (B) had an I_S value of 66 emu/gm, no detectable αFe_2O_3 and no extra non cubic X-ray lines. Sample E (500°C) and F (600°C) were red and showed only αFe_2O_3 in the X-ray pattern. However, the reflectance of E at $\lambda > 1.2$ μm was considerably reduced compared to F. E had an I_S value of ~ 6 emu/gm compared to F with I_S ~ emu/gm. Both E and F had the 0.87 μm Fe^{3+} absorption feature.

The characteristic features for $\alpha FeOOH$, αFe_2O_3 and γFe_2O_3 over the range 0.5 to 1.2 μm are indicated in Figure 1C. This figure illustrates the reflectance curves observed before and after thermal conversion (600°C - 2 hours in air) of both $\alpha FeOOH$ (YLO 1988 pigment) and γFe_2O_3 to αFe_2O_3. Beneath the curves are letters a, b, and c.

a - is the feature observed as a band at 0.64 μm in synthetic $\alpha FeOOH$, but usually recorded as a distinct shoulder in most natural samples. This feature flattens the spectrum between 0.6 and 0.75 μm when FeOOH is dominant.

b- is the 0.85 - 0.87 μm absorption feature observed for αFe_2O_3.

c- is the ~ 0.9 μm feature observed in γFe_2O_3 and FeOOH, and actually may extend out to 0.94 μm depending on experimental variables, i.e., method of preparation, presence of absence of a superlattice in γFe_2O_3 etc. This will be considered below.

By X-ray diffraction analysis several specific γFe_2O_3 types are recognized, due to the presence or absence of non-magnetite lines (see Bernal et al., 1958). These are superlattice lines and their presence or absence depends on the method of preparation - for example:

$\alpha FeOOH \rightarrow \alpha Fe_2O_3 \rightarrow Fe_3O_4 \rightarrow \gamma Fe_2O_3$ (the normal method of preparation for recording media), $Fe(OH)_2 \rightarrow \gamma Fe_2O_3$, and $\gamma FeOOH \rightarrow \gamma Fe_2O_3$ all have different X-ray patterns. Table 1 lists some of the properties of γFe_2O_3 samples used in this study - the X-ray patterns are shown in Figure 4. Peaks having black dots above them are the non-cubic extra lines. All of the samples listed in Table 1 show extra non-cubic lines. Only the γFe_2O_3 produced by oxidation of 7029 (see Figure 1b and Figure 3) had the cubic pattern with reduced cell size as expected for γFe_2O_3. This γ phase had a distinct dark brown color. All of the γFe_2O_3 samples listed in Table 1 converted to αFe_2O_3 on heating for 1 hour at 600°C, developing the characteristic 0.87 μm Fe^{3+} absorption feature. Thermomagnetic curves for the γFe_2O_3 samples and for size graded Fe_3O_4 (produced by grinding bulk material) are shown in Figure 5. On heating to 650° in approximately 1 hour (H = 3000 oe), and then turning off the furnace to cool, all γFe_2O_3 samples converted to αFe_2O_3 (determined by X-ray and reflectance curves). Note that the curve shapes are different. 2530 and 5029 show an almost linear decrease in magnetization with temperature out to ~ 525°C after which the magnetization drops off sharply on continued heating. In 2035 the decrease in linear out to ~ 400°C after which the magnetization curves smoothly to zero. In 9853 the magnetization decreases continuously and

smoothly to zero. Note that 2530 and 5029 (Table 1) have similar coercivities and as we shall see their reflectance curves are similar, while 9853 and 2035 are different from each other and from 2035-2530. Thus while not establishing the origin of the differences, all data demonstrate the distinctive aspects of different γFe_2O_3's, i.e., both magnetic and spectral differences.

γFe_2O_3 reflection spectra are shown in Figure 6A. The Fe^{3+} absorption feature is located ~ 0.92 μm. 2530 and 5029 are almost identical while 2035 and 9053 have different shapes and the Fe^{3+} feature is shifted to slightly higher λ. Heating 5029 and 2530 for 1 hour at 200°C produced no X-ray detectable αFe_2O_3 but did shift the position of the Fe^{3+} feature to slightly higher λ suggesting a re-ordering phenomena affecting the Fe^{3+} environment. The shift in the Fe^{3+} feature was greater for 2530 and the reflectance decreased dramatically, flattening between 1.2 μm and 1.7 μm after which a linear increase with λ was recorded.

In Figure 6B it is seen that both αFe_2O_3 and αFeOOH flatten between 1.2 and 1.3 μm while γFe_2O_3 does not until 1.5 μm. αFe_2O_3 remains continuous and more or less flat or slopes smoothly and slightly downward beyond 1.2 μm (see Figure 6A), γFe_2O_3 changes abruptly between 1.7 and 1.85 μm sloping upward out to 2.4 μm or remaining flat beyond 2.0 μm (Figure 6A). αFeOOH slopes downward beyond 2.1 μm producing a dome shape between 1.2 and 2.4 μm.

Characteristics of the FeOOH, αFe_2O_3 and γFe_2O_3 spectra are summarized in Figure 6B. Figure 6B presents two sets of spectra (a) - αFeOOH and αFeOOH heated 2 hours at 600°C (= αFe_2O_3) and (b) γFe_2O_3 (2530) and the same heated at 500°C for 1 hour and 600° for 1 hour (= αFe_2O_3). In each case the ~ 0.92 μm absorption shifts to 0.87 μm

on conversion to αFe_2O_3 (X-ray identification). Comparing the ratio of reflectance (R) at 0.6 μm to that at 0.75 μm (Table 2) separates FeOOH from α or γFe_2O_3 since it considers the 0.64 μm feature. The ratio R (1.0 μm) to R (1.2 μm) considers the change in slope between 1.0 μm and 1.2 μm and separates γFe_2O_3 from αFe_2O_3 and αFeOOH. Note that the absorption is more intense for αFe_2O_3 than for γFe_2O_3 and the 'bright peak' shifts from ~ 0.8 μm to 0.75 μm on $\gamma \rightarrow \alpha Fe_2O_3$ conversion. The specific absorption features for αFe_2O_3, γFe_2O_3, and αFeOOH are identified in Figure 6B.

IRON OXIDE DIAGNOSTICS (SYNTHETICS) (see Table 3)

	Fe^{3+} feature	'bright feature'	R(0.6)/R(0.75)	R(1.0)/R(.12)
αFe_2O_3	0.87 μm*	~ 0.75 μm*	~ 0.50	~ 0.58
γFe_2O_3	0.92-0.94μm*	~ 0.80 μm*	~ 0.92	~ 0.72*
αFeOOH	0.64* and 0.90-0.92 μm*	~ 0.77 μm	~ 0.85*	~ 0.60

Curve shape beyond 1.2 μm

αFe_2O_3 - turnover at 1.2 μm and essentially flat or slight linear decrease with λ out to 2.4 μm

αFeOOH - turnover at ~ 1.25 μm, flattens at ~ 1.3 μm describing a gentle dome out to 2.4 μm

γFe_2O_3 - turnover to flatten at 1.5 μm, flat response out to between 1.7 to 1.85 μm then abrupt slope change upward to ~ 1.9 μm and thereafter continuously increasing reflectance out to 2.4 μm.

Natural materials present specific variations on the above since the natural samples are never simple one component, highly cyrstalline,

grain size sorted surfaces. For FeOOH, 'yellow' natural surfaces, the region between 0.6 and 0.75 is best described as a stepped plateau with the dip at 0.64 μm instead of the well developed 0.64 μm 'band'. The presence of clays and water modify the curve shape out to 2.4 μm, as described earlier in this paper, and may dominate the shape from 1.2 to 2.4 μm.

KBr pellet absorption spectra presented by Liese (1969) and Kodama (1977) (6 μm out to 33 μm) provide additional evidence for the spectral uniqueness of iron oxides (Figure 7).

NATURAL SAMPLES

Rock Surfaces - In real situations it is uncommon to find rock surfaces which are unaltered. In our studies the working definitions of rock surface state are as follows: fresh surface - a saw cut face or broken surface showing absence of iron oxide weathering. The rock type can be identified and primary mineralogy and texture ascertained when grain size is sufficiently large. The level of reflectance is determined by rock basicity. Stained surface - all recognition characteristics are the same as for the fresh surface. (This surface is analagous to stained wood.) The reflection spectrum is that due to the rock type plus a stain overprint which 'colors' the rock. The maximum effect is noted for acidic rocks. Coated surface - a coating, which is analagous to painted wood, renders visual rock identification impossible. The reflection spectrum is due mainly to the makeup of the coating.

A plate ~ 1 cm thick was cut from a granitic hand sample about 10 cm x 10 cm x 20 cm collected by Dr. R. D. Warner from the Idaho Batholith. From the adjacent remaining bulk sample, surface slices several mm thick

were removed, corresponding to the locations 33, 34, 35, 36 shown in Figure 8A. The location of the light and dense iron stain, and no stain regions of the slice are indicated. Specimens 33 and 34 had stained surfaces, the SiO_2, feldspar and mafics were clearly identifiable, while specimens 35 and 36 were coated with a dense iron oxide. The scanning electron micrographs (Figure 9) of the surfaces of 33 (A,B) and 36 (C,D) document the difference between stained and coated surfaces. Crystalline surfaces are visible in A and B, qualitative EDAX spectra identifies Fe, Ca, Al, etc. while in C and D, which shows no evidence of crystalline faces and an 'amorphous'-globular surface, only Fe is identified in the EDAX spectra. The reflectance spectra for 33, 34, 35 and 36, and the fresh surface are shown in Figure 8B.

A thin strip was cut from the plate as indicated in Figure 8A and the strip was cut into blocks A to H. An arbitrary X-Y-Z orientation system with sense as indicated was transferred to each block. Figure 8C is the magnetometer record of the NRM (natural remanent magnetization) for the blocks. Block A includes the 33 stained surface and is iron stained over half the volume, B, C and D are unstained, and from Block E to H the stain becomes increasingly more dense -- block H includes surface 36. The SIRM (saturation isothermal remance; H = 8400 oe) record is indicated below the NRM record. The effect of terrestrial weathering on magnetic properties is always significant as indicated. The full 0.5 to 2.4 μm spectra for 33, 34, 35 and 36 and the spectrum from a fresh surface are shown in Figure 10. The fresh rock surface for this granitic rock shows an almost constant level of reflectance at $\sim$ 40%. The dome shape to the curves between 1.2 and 2.4 μm can be due to

(a) moisture, (b) clays (see Lindberg & Snyder, 1968) and (c) FeOOH. Note in Figure 10, the corroded meteorite surface (labeiled corrosion surface) has little moisture and no clays and the dome shape disappears. The presence of clays would also tend to soften absorption features below 1.2 μm as the spectra are flat and have high reflectance in this region. Comparing 33 and 34 it is immediately apparent that the 0.9 μm absorption is deeper in 34 than 33, the bright peak is developed and absorption is stronger below 0.6 μm.

QUALITATIVE EVALUATION OF CLAY IN THE PRESENCE OF Fe OXIDES

We shall consider the region 0.5 to 1.2 μm since telescope curves, LANDSAT imagery and Viking lander multispectral data are recorded in this range. In Figure 10 along with the gibbsite and kaolin spectra acquired as part of this study, the NONTRONITE SPECTRUM of Lindberg and Snyder (1972) has been copied, i.e., we picked the reflectance at each 0.1 μm, from 0.5 μm and then drew a smooth curve beteen the points. From 0.5 to 1.1 μm the Nontronite Spectrum has the same general shape as FeOOH. In the region between 0.6 μm and 0.75 μm αFe_2O_3 and γFe_2O_3 are strongly absorbing. If FeOOH were present, strong absorption would be noted between 0.5 and 0.6 μm -- this is not observed for nontronite. Though Lindberg and Snyder did not perform hydration experiments with nontronite, experiments with Montmorillonite did demonstrate that the reflectance spectrum is strongly dependent on the state of hydration. Of the clays they studied only the montmorillonites showed significant strong absorption between 0.5 and 0.9 μm after dehydration. If a montmorillonite clay is present at the Martian surface it follows that the clay not only

must be iron rich but in a very low state of hydration. Adams and McCord (1969) found that it was not possible to model the Mars telescope curve by adding FeOOH to powdered basalt; they would experience the same problem with Nontronite, but to a greater degree, because of the high reflectance below 0.6 μm. Note also that dehydration flattens the clay curves beyond 1.2 μm (Lindberg and Snyder, 1968) eliminating the dome shape as mentioned earlier.

ROCK TYPES - As shown previously a fresh granitic rock has a reflectivity of ~ 40% (Figure 10). A fresh granodiorite (from the Glen Alpine Stock (Peikert, 1964) has a reflectivity of ~ 30% as shown in Figure 11A (98A). Stained surfaces (20B, 23C) show higher reflectivity and stronger absorption below 0.75 μm, but show no strong evidence of the Fe^{3+} absorption feature. Figure 11B shows reflection spectra for 200 mesh powders from a series of GAS powders chosen visually to represent degree of weathering. (G1A was deep reddish brown and G105 was gray.) The surface spectra and rock powder spectra are distinctly different. The reflectance ratio R(0.5 μm)/R(0.9 μm) varies from 0.9 to 0.5 as the initial magnetic susceptibility varies from 34.9×10^{-4} emu/gm to 4.12×10^{-4} emu/gm. This is associated with oxidation of Fe_3O_4. Pertinent data on the GAS powders and GAS98 and GAS20 surfaces are listed in Table 3.

Fresh Diorites exhibit a constant reflectivity of ~ 20% (Figure 12A). Surfaces from two hand samples were removed and their spectra were acquired (Figure 12A) - Table 3 lists the surface state and NRM values for each surface. Fresh ultra-basic rocks (Lizardite, Serpentinite) exhibit a constant reflectivity of ~ 10% (Figure 12B). Though we have

certainly not completed a systemmatic study of rock surfaces -- this was not the purpose of this study -- it appears that from rock surfaces: that reflectance increases with increasing acidity, that fresh rock surfaces show essentially flat spectra, that the significant alterations are related to stains and coatings and that the magnitude of the effects of stains and coatings increase with rock acidity. An interesting point observed in the reflection spectra from all rock surfaces studied is that only in the granitic rock was the $\sim$ 0.9 μm Fe^{3+} feature well developed.

MIXTURES: CLAYS AND SOILS - Potters nurture clay through various 'mystical' stages before their end product is realized. The plastic clay the potter begins with is refined and homogeneous, care being taken to remove sulfides, carbonaceous material and iron particles. Shown in Figure 13 is a spectrum of a plastic clay surface, dried to the 'leather hard' stage. The smooth dome shape with the water bands is typical. Prior to glazing, the body is next 'Bisque fired', at $\sim 700^{o}C$ in flowing air. As the spectrum illustrates the αFe_2O_3 characteristics of the resultant light pink body are clearly evident, i.e., the 0.87 μm Fe^{3+} feature, the flattening of the curve (which may also be due to dehydration) out to 2.4 μm, the small bright peak at 0.75 μm, and the strong absorption below 0.6 μm.

A series of 6 loam soils from the State of Maryland were obtained from the University of Maryland Agronomy Department. The soils have been well characterized by members of the Department. Table 4 lists some of the characteristics of these soils. Spectra for the soils are shown in Figure 14 along with spectra from a white sandstone surface

and a clay coated (natural surface) limestone surface. The soils are divided into 3 groups (see Table 4) on the basis of their curve shapes. The free iron vs. clay content of the soils is plotted in Figure 15 along with the initial susceptibility (χ_o) values from Table 4. There is an excellent correlation between free iron, χ_o, and the clay content. The only exception is the Penn loam, the large χ_o value is due to the fact that only from this soil was it possible to remove large particles with a hand magnet which is consistent with the presence of large multidomain particles.

The 0.9 μm absorption in the soil spectra groups is intensified as the free iron content increases. From this figure it is clear that it is difficult to distinguish among loamy soils, a sandstone surface, and a weathered limestone surface and more detailed studies are required to indicate which spectral ranges are best for discrimination.

COLORED IRON ORES AND CORROSION PRODUCTS

A series of sample powders from the metamorphosed Biwabik formation were obtained (French, 1965) and these were studied to test the applicability of the Fe oxide diagnostic features in qualitatively characterizing samples of simple mixed mineralogies. Table 5 lists some of the properties of samples whose reflectance spectra are presented in Figure 16A. Samples containing αFe_2O_3 (113 and 33) have the 0.87 μm Fe^{3+} feature and the bright peak at 0.75 μm (compare these spectra to Figure 14). The yellow sample (91) has the 0.9 μm Fe^{3+} feature. Sample 146 contains no αFe_2O_3 or FeOOH and shows none of the Fe^{3+} absorption features.

Kilograms of meteoritic 'shale' were picked from one of the Campo del Cielo meteorites recovered by Dr. William Cassidy. The material was hand picked to provide visually distinct yellow, red and brown fractions. The material was then subjected to hand magnet separation which further enhanced the color purity of the non-magnetic fractions, resulting in extracted magnetic brown material. Spectra for the fractions are shown in Figure 16B. The yellow and brown non-magnetic fractions have the 0.9 μm Fe^{3+} feature while the red fraction has this feature near 0.87 μm. The colored non-magnetic material had higher reflectance at all wavelengths and well developed Fe^{3+} features compared to magnetic fractions.

BASALTIC ROCK POWDERS

A series of chemically analyzed Puerto Rico Trench basaltic rock powders (400 mesh) were obtained from Dr. Andrew Nalwalk. Spectra for the Class I and Class II rocks (Wasilewski, 1968) are shown in Figure 17A. The Class I rock (02017) contains optically homogeneous titanomagnetite, with an oxidation index ($Fe^{2+}/Fe^{2+}+Fe^{3+}$) of 0.27 and the powder is a gray color. Beneath the spectra the relevant magnetic properties for both rocks are listed. The thermomagnetic characteristics of both classes of rocks are summarized in Figure 17B. The H_2O^+ content of Class I rocks is 1.12 ± 0.22 and for Class II rocks is 2.33 ± 0.41. The dashed spectral curves in Figure 17A are those obtained after heating the powders in air at 600°C for 2 hours. The 1 μm feature shifts to slightly lower λ after heating. The Class II rocks have higher reflectivity initially and the difference on heating is greatest for Class II rocks, the contrast between the heated and unheated samples is significant in the region 0.5 to 0.9 μm.

METEORITE-ASTEROID MATCHES

Chapman and Salisbury (1973) and more recently Gaffey (1976) have measured laboratory reflectance spectra for nearly all meteorite groups. Gaffey (1976) concludes "It has been shown that each meteorite type representing a particular mineral assemblage and metamorphic grade has a characteristic reflectance curve and that spectral characteristics can be understood in terms of the type, composition, relative abundance and distribution of the constituent mineral phases". Each group of meteorites also has a distinctive range of magnetic properties (Wasilewski, 1975). The main thrust in measuring laboratory reflectance curves of meteorites has been to attempt to match these curves with telescope reflectivity curves of asteroids. Therefore, once such a match is made we can specify within close limits the magnetic properties of the asteroid. Figure 18A is a plot of χ_o (the initial susceptibility) vs wt % Fe + Ni. (This data is from the Russian literature -- see Guskova, 1974). The high χ_o values for Enstatite chondrites is related to the large metal grain size and Si content of the metal. Figure 18B is a plot of χ_o vs Petrologic Class for the ordinary chondrites. The spectral curve parameters of Chapman and Salisbury (1973) are included to indicate the systematic variation in the spectral and magnetic data.

COMMENTS ON MARS

The Martian surface appears to be yellowish brown (Huck et al., 1977). This is consistent with the presence of FeOOH providing the color is due only to a discrete iron species. According to Binder et al., (1977) this is also consistent with a model requiring a limonite strain, on the rock blocks and fines, formed by chemical weathering of mafic minerals in igneous rocks. Binder and Cruikshank (1964) consider the

limonite to be derived from chemical weathering in an earlier epoch when H_2O and O_2 were more abundant in the Martian atmosphere. Huguenin (1974) on the other hand argues that UV photo-stimulated oxidation of mafic minerals under present Martian conditions could be responsible. Huck et al. (1977) on the basis of their spectral reflectance measurements consider that Fe rich montmorillonite (nontronite) might be present.

Spectral reflectance estimates of limonite (Huck et al. 1977, Figure 4d), miss the distinctive 0.64 μm feature for FeOOH, present to noticeable extent in all limonites (see Figure 6 and 10). Likewise the FeOOH estimate 'peak' is located at 0.75 μm, while 'estimates' (Figure 7 in Huck et al. 1977) for surface locations definitely position the hump at ~ 0.8 μm. Thus the data currently available leaves unresolved any correct designation of a particular species responsible for the yellow brown color of Mars.

Examination of the nontronite spectrum (e.g., Lindberg et al. 1972 and Figure 10) reveals a similarity to FeOOH in the region 0.6-0.75 μm. The strong absorption below 0.6 μm for FeOOH - compared to nontronite- makes these species discernable. Clark et al. (1976) discussed the point that the chemical data is inconsistent with a continuous Fe oxide coating more than 0.25 μm thick on the silicates and that most of the oxides must exist as discrete grains or inclusions within silicates. Hargraves et al. (1977), concluded that the bulk of particles clinging to the magnets are in fact composite, each containing a small percentage of highly magnetic material. In view of the supposed composite nature of attracted magnetic particles, the lack of definitive

spectral information, and the various possibilities for the source of Martian surface coloration, e.g., photostimulated oxidation and possibly dehydration (Huguenin, 1973) and nontronite dehydration (MacKenzie and Rogers, 1977), it would appear difficult to identify particles attracted to the lander magnets. However, based on color of composites grains alone and the magnetic attraction, any magnetic species is possible. If the species attracted to the magnets were discrete grains and no significant surface coating existed then magnetic attraction and color would indicate γFe_2O_3.

CONCLUSIONS

Individuals interpreting LANDSAT imagery should find available spectral data inadequate for interpretation primarily because the rock powder data, mineral mixtures etc. do not represent the true imaged surfaces.

A rock powder is not a representation of the rock surface, and a soil no matter how it is derived is not represented by rock powders or simple mineral mixtures. Even for the lunar surface a powdered rock is a totally inadequate representation to a telescope curve. In remote sensing of solid solar system bodies the natural weathering environment appears to be the most important factor in determining surface spectra.

In this paper the spectra and magnetic diagnostics for the common Fe weathering products have been described, and the importance of the type of weathering surface has been adequately outlined. Examples support a simple two component model for remote sensing of terrestrial

surfaces, as Fe weathering products and clays, though in reality the surface mineralogy may consist of carbonates, sulfates and other transition metal products as well as SiO_2 and Al_2O_3 etc.

Magnetic properties have been emphasized for two primary reasons: (a) they can be used to evaluate the weathering surfaces and monitor the depth of weathering. In our examples, the stained rock surfaces have substrates (down to several mm) which are less altered magnetically than the substrate beneath a coated surface. (b) Future NASA planetary missions may include experiments which provide spectral and magnetic data. Therefore it is important to have a data base in order to maximize interpretive capability. This report represents a beginning in this direction.

REFERENCES

Adams, J.B. and A.L. Felice, 1967; Spectral Reflectance 0.4 to 2.0 Microns of Silicate Rock Powders, J. Geophys. Res. 72, 5705.

Adams, J.B., and T.B. McCord, 1969, Mars: Interpretation of Spectral Reflectivity of Light & Dark Regions, J. Geophys. Res., 74, 4851.

Bernal, T.D., D.R. Dasgupta and A.L. Malkay, 1959, The Oxides and Hydroxides of Iron and Their Structural Relationship, Clay Minerals Bull., 4, 15.

Binder, A.B., R.E. Arvidson, E.A. Gunness, K.L. Jones, E.C. Morris, T.A. Mutch, D.C. Pieri and C. Sagan, 1977, The Geology of the Viking Lander 1 Site, J. Geophys. Res., 82, 4439.

Chapman, C.R. and J.W. Salisbury, 1973, Comparisons ofMeteorite and Asteroid Spectral Reflectivity, Icarus, 19, 507.

Clark, B.C., A.K. Baird, H.J. Rose, P. Tanlmin III, K. Keil, A.J. Castro, W.C. Kelliker, C.D. Rowe, P. H. Evans, Inorganic Analyses of Martian Surface Samples at the Viking Landing Sites, Science, 194, 1283.

French, B., 1964, Stability of Siderite, $FeCO_3$, and Progressive Metamorphism of Iron Formation, Ph.D. thesis, Johns Hopkins University.

Gaffey, M.J., 1976, Spectral Reflectance Characteristics of the Meteorite Classes, J. Geophys. Res., 81, 905.

Guskova, Ye. G., 1972, The Magnetic Properties of Meteorites (MAGNITNYYE SVOYSTVA METEORITOV), NASA Technical Translation, NASA TT F-792.

Hargraves, R.B., D.W. Collinson, R.E. Arvidson, and C.R. Spitzer, 1977, The Viking Magnetic Properties Experiment in Primary Mission Results, J. Geophys. Res., 82, 4547.

Huck, F.O., D.J. Jobson, S.K. Park, S.D. Wall, R.E. Arvidson, W.R. Patterson, W.D. Benton, 1977, Spectrophotometric and Color Estimates of the Viking Lander Sites, J. Geophys. Res., 82, 4401.

Huguenin, R.L., 1974, The Formation of Geothite and Hydrated Clay Minerals on Mars, J. Geophys. Res., 79, 3895.

Hunt, G.R., J.W. Salisbury and C.J. Lenhoff, 1971, Visible and Near-Infrared Spectra of Minerals and Rocks, III Oxides and Hydroxides, Mod. Geol. 2, 195,

Hunt, G.R., J.W. Salisbury and C.J. Lenhoff, 1973a, VII Acadic Igneous Rocks, Mod. Geol. 4, 217.

Hunt, G.R., J.W. Salisbury and C.J. Lenhoff, 1973b, VIII, Intermediate Igneous Rocks, Mod. Geol, 4, 237.

Hunt, G.R., J.W. Salisbury and C.J. Lenhoff, 19 ,c, IX Basic and Ultra-basic Igneous Rocks, Mod. Geol. 5, 15.

Kodama, H., J.A. McKeague, R.J. Tremblay, J.R. Gosselin, and M.G. Townsend, 1977, Characterization of Iron Oxide Compounds in Soils by Mossbauer and Other Methods, Can. Jun. Earth Science, 14, 1.

Liese, H.C., 1967, An Infrared Absorption Analysis of Magnetite, Amer. Min., 52, 198.

Lindberg, J.D. and D.G. Snyder, 1972, Diffuse Reflectance Spectra of Several Clay Minerals, Amer. Miner. 57, 485.

Peikert, E.W., 1965, Model for Three Dimensional Mineralogical Variation in Granitic Plutons Based on the Glen Alpine Stock, Sierra Nevada, Califonria, Geol. Soc. Amer. Bull, 76, 331.

Wasilewski, P.J., 1968, Magnetization of Ocean Basalts, J. Geomag. Geoelec., 20, 129.

Wasilewski, P.J., 1974, Magnetochemical Properties of Bodies in the Solar System Derived from Spectral Reflectivity Curves, Meteoritics, V9, 416.

TABLE 1

Properties of γFe_2O_3 Samples Used in this Study (C.K. Williams & Co. MO Series)

SPECIMEN #	COLOR		PARTICLE SHAPE	H_c (oe)
2035	yellow brown	0.2 μm	acicular	345-365
2530	yellow brown	0.2 μm	acicular	385-305
5029	yellow brown	0.5 μm	acicular	275-300
9853	brown	0.05 μm	cubic	515-555

TABLE 2

Reflectance (R) Ratio for $\alpha FeOOH$, γFe_2O_3 and αFe_2O_3

	$\alpha FeOOH$	γFe_2O_3	αFe_2O_3
R(0.6 μm)/R(0.75 μm)	0.85	0.42	0.50
R(1.0 μm)/R(1.2 μm)	0.60	0.72	0.58

Table 3 - Magnetic And Spectral Curve Diagnostics for Synthetic Iron Oxides

Species	T_M	M(emu/gm)	Color	Fe^{3+} Feature & Curve Shape
Fe	1050 K	218	--	none - slope increases with λ
FeO	198 K	--AF	--	none
Fe_3O_4	850 K	96	black	none - flat curve with shallow and broad 1 μm feature
γFe_2O_3	~870 K[1]	66-76	brown	0.90 μm - curve shape diagnostic[3]
αFe_2O_3	950 K	0.5	red	0.87 μm[3]
αFeOOH	~200 K[+/-]	--AF[2]	yellow	0.64 μm + 0.90 μm[3]

T_M - Magnetic transition temperature

M - Magnetic moment, AF = antiferromagnetic

1 - At this temperature γFe_2O_3 (brown) converts to αFe_2O_3 (red)

2 - Pure αFeOOH should be antiferromagnetic, however, some species studied do have moments < 10 emu/gm. The other FeOOH species (β, γ) may have moments < 20 emu/gm.

3 - See Figure 6 and 10 for curve shapes.

TABLE 4

Magnetic Data on Glen Alpine Stock (GAS) Granodiorite Surfaces and Powders and RW Diorite Surfaces

GAS Surfaces

Specimen	Surface	NRM
GAS 98	Fresh	0.266×10^{-4} emu/gm
GAS 20	Stain	1.922×10^{-4} emu/gm

GAS Powders

Specimen	Color	χ_o 10^{-4} emu/gm
G105A	Gray	34.87
G19A	Reddish	13.02
G11A	Reddish brown	9.95
G1A	Deep reddish brown	4.12

RW Dionite Surfaces

Specimen	Surface	NRM
16	Fresh	1.88×10^{-4} emu/gm
15	Stain	2.93
14	Dense stain	19.56
13	Coating	21.28

NOTE: The magnetic susceptibility and saturation magnetization values decrease and the NRM values increase with weathering.

TABLE 5

Properties of Maryland Loam Soils (Ap Horizon)

Soil	Color	Free Fe	χ (10^{-3} emu)	Sand	Silt	Clay
Manor	Dark red brown	1.95	5.27	35	38	27
Hagerstown	Dark red brown	2.16	4.76	42	30	28
Myersville	Yellow	1.52	2.72	9.5	70.4	20.1
Neshaminy	Yellow	1.63	3.40	49.5	32.2	18.3
Matapeake	Brown-dark brown	0.65	2.21	26.2	63.4	10.4
Penn	Dark red brown	0.84	10.54	28.9	53.8	17.3

Table 6

Properties of Biwabik Formation Samples

Sample	Color	I_S	SiO_2	Fe_2O_3	Fe_3O_4
146	Gray	9.2	--	--	--
113	Deep Red	29.42	40-50	5-10	10-20
33	Pink	--	90.95	5-10	2-5
91	Yellow	3.04	--	--	--

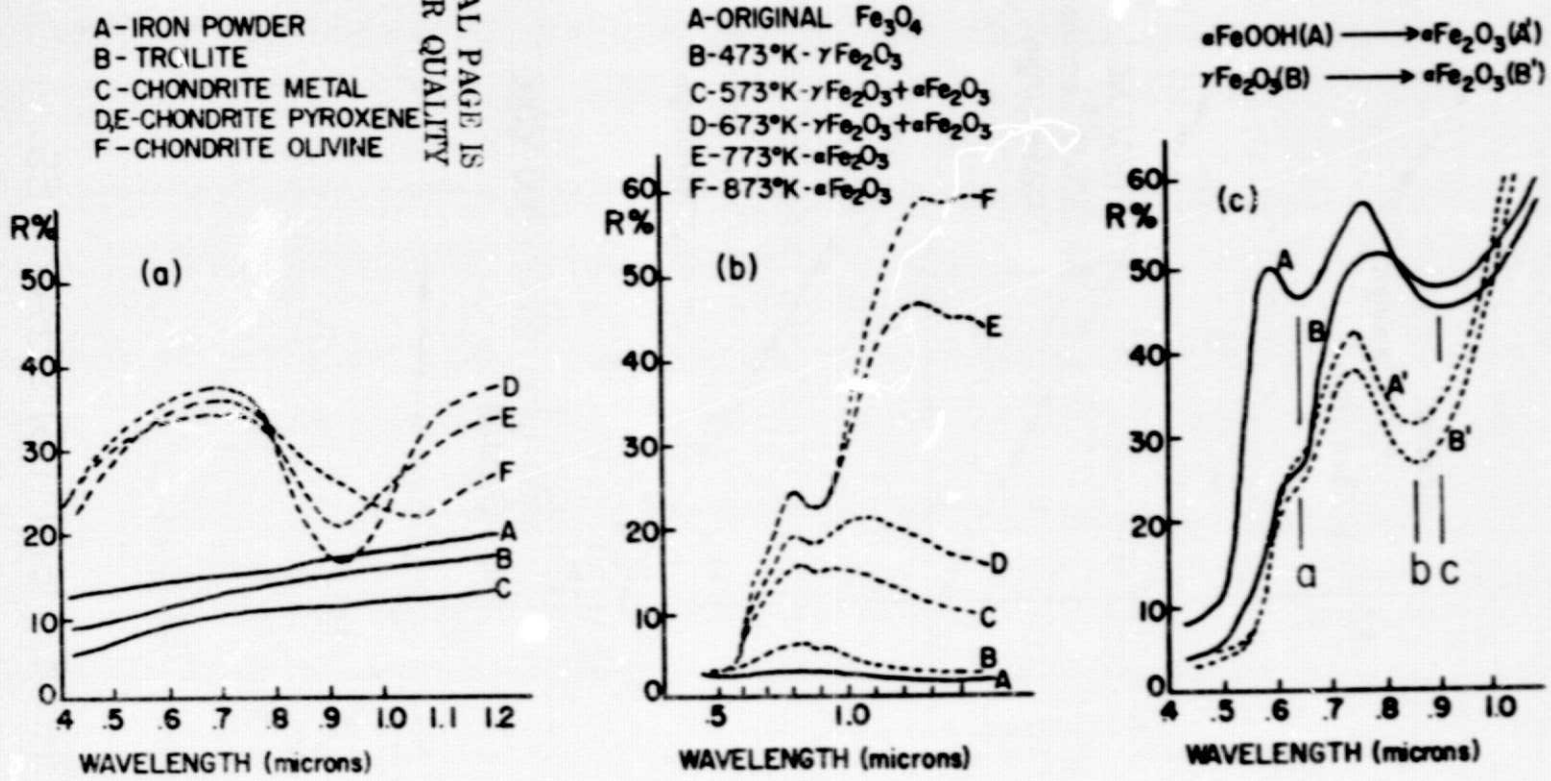

Figure 1. (from Wasilewski, 1974)

(a) reflectance curves for Bruderheim (L6) separates and iron powder, (b) reflectance curves illustrating the changes associated with oxidation of Fe_3O_4 (see text for description of experiment), (c) reflectance curves demonstrating the differences between αFeOOH, and γFe_2O_3 and the product αFe_2O_3 after thermal conversion.

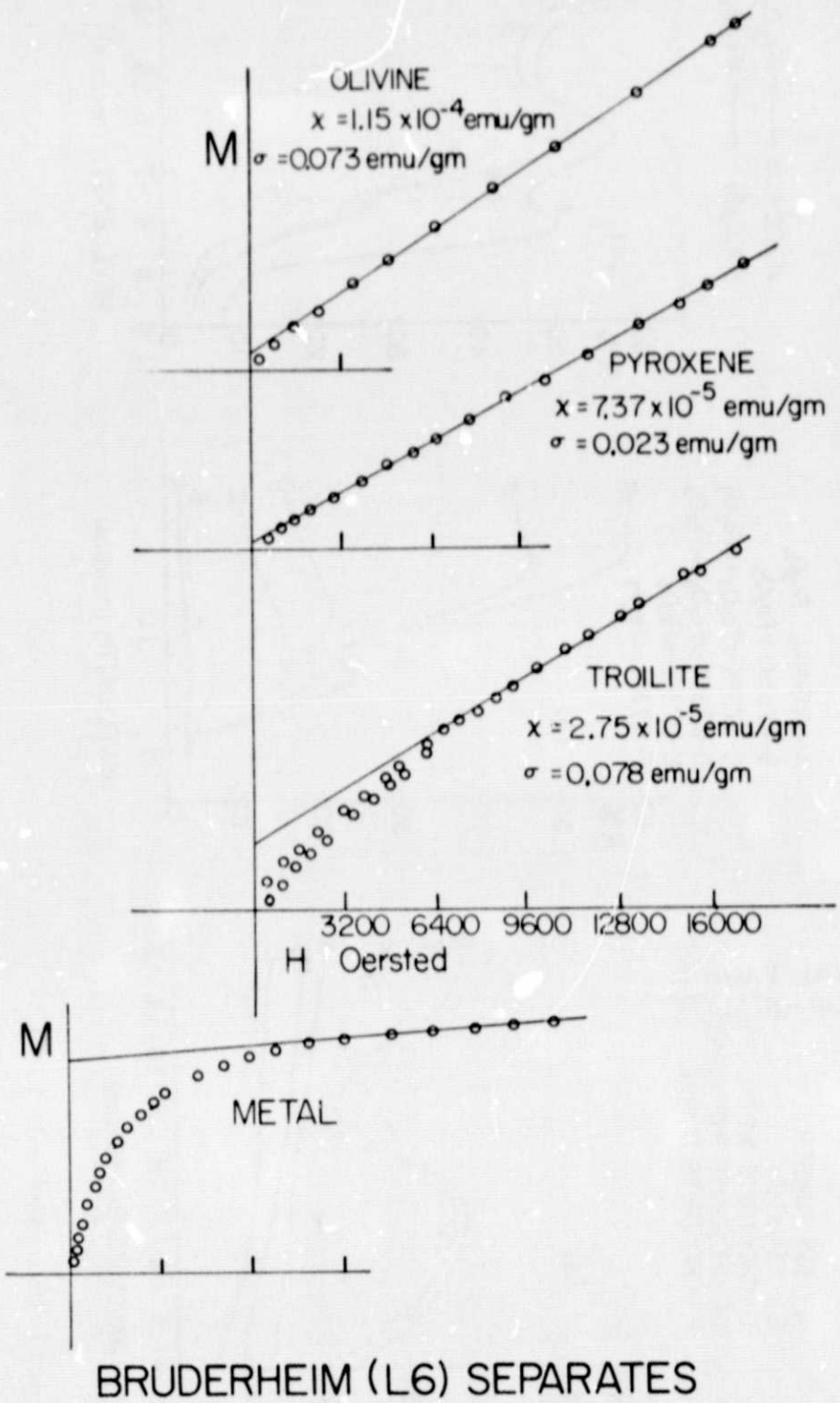

Figure 2. Magnetic hysteresis loops for Bruderheim separates (measured at 78 K).

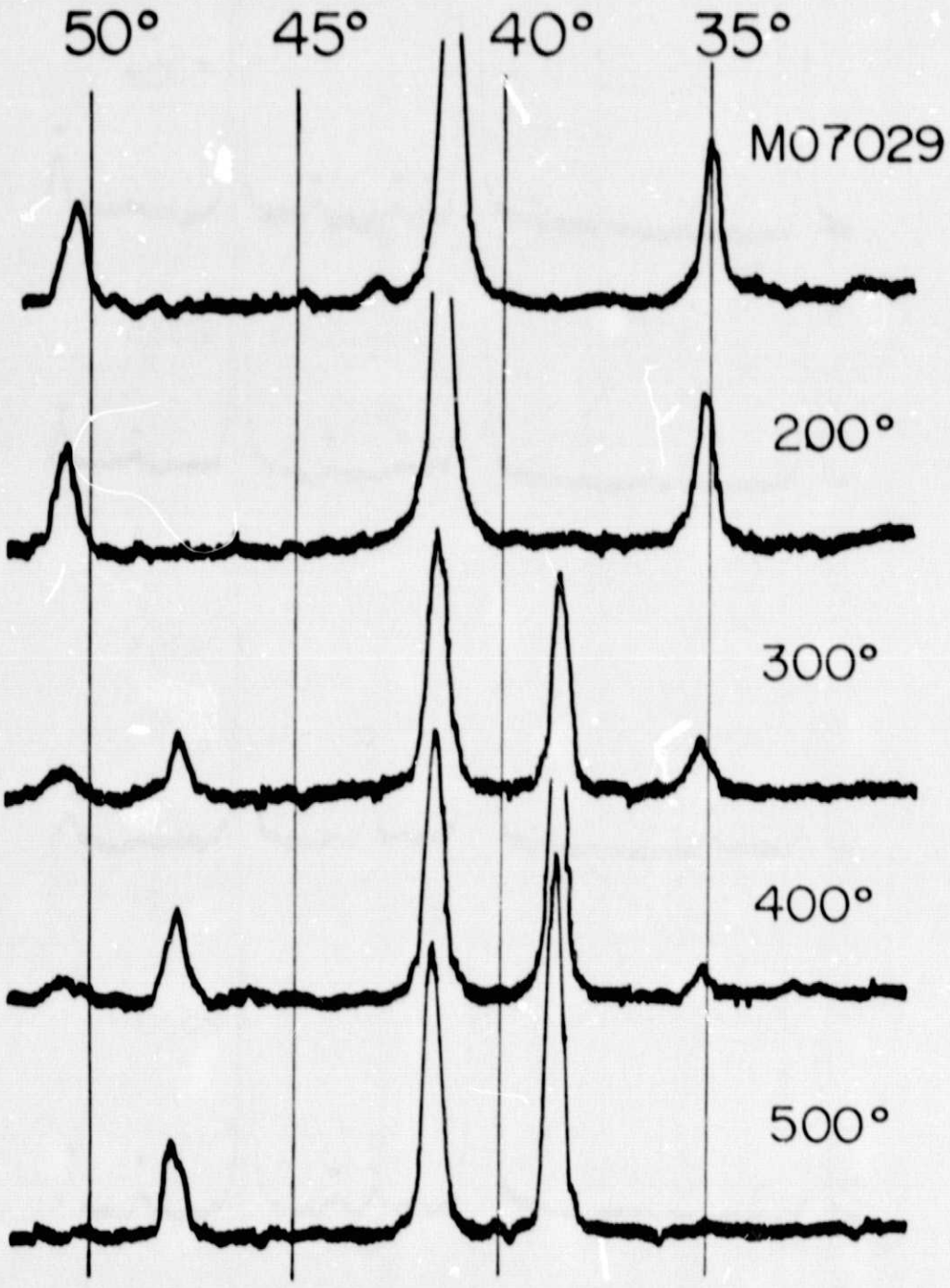

Figure 3. X-ray spectra obtained on a Norelco diffractometer using iron filtered Cobalt radiation. Numbers at top of vertical lines are degrees 2θ. These are same samples as in Figure 1b.

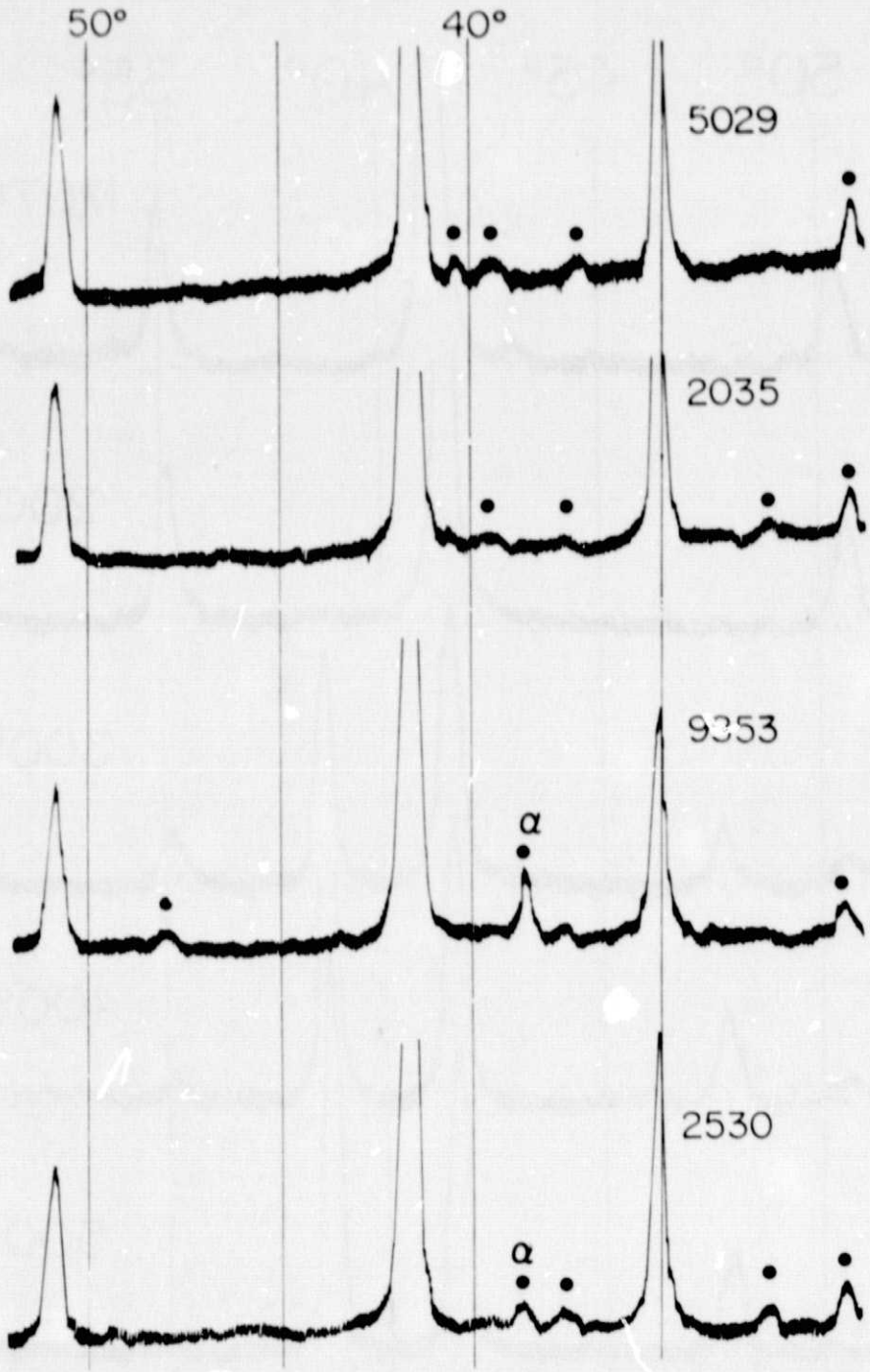

Figure 4. X-ray spectra for Maghemites (γFe_2O_3). Numbers at top of vertical lines are degrees 2θ. Black dots above peaks identify extra non-cubic lines, α above extra peaks indicates αFe_2O_3.

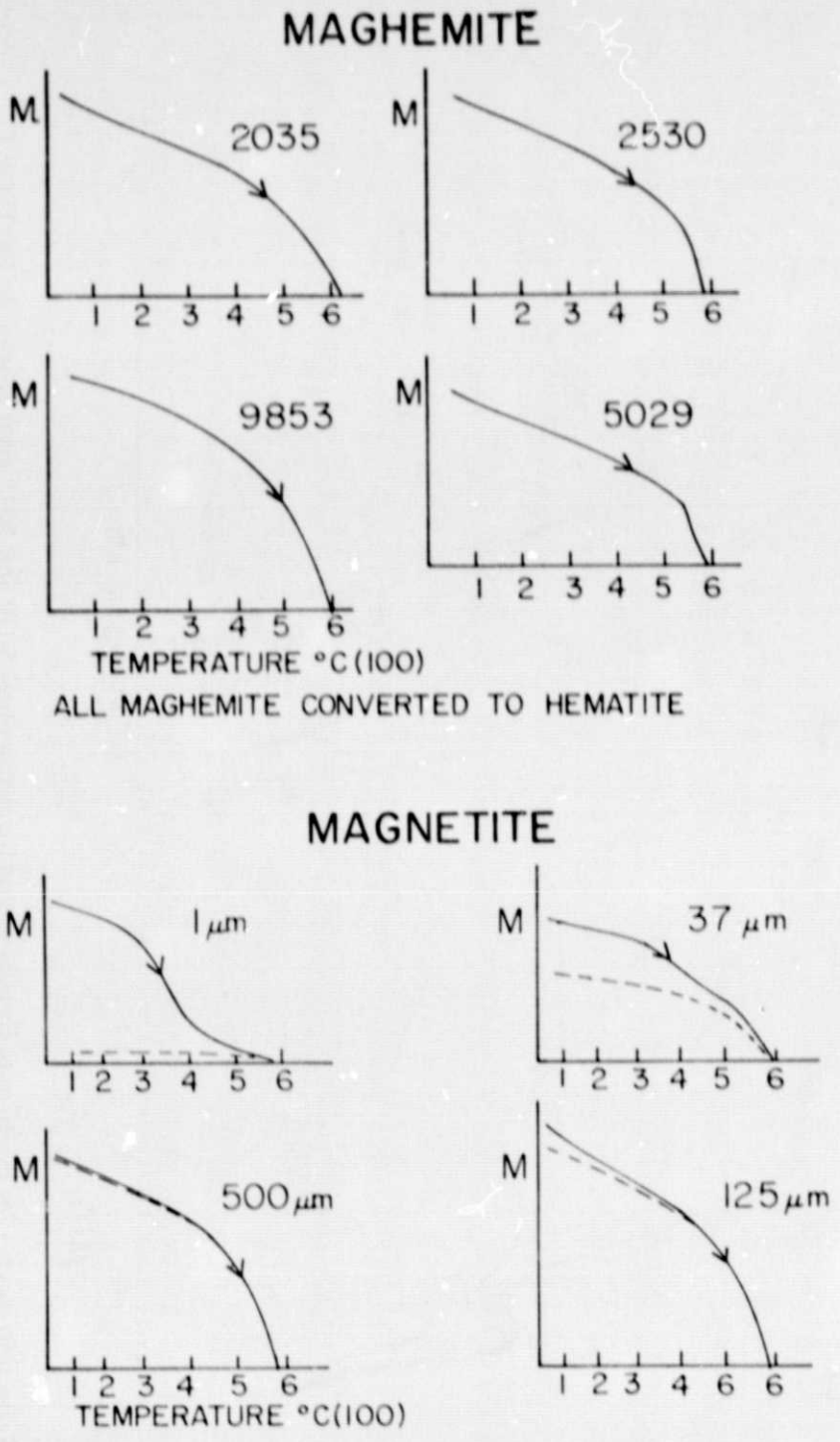

Figure 5. Thermomagnetic curves for maghemite and size graded Fe_3O_4 powders. (Heating to 650°C in approximately 1 hour in air.)

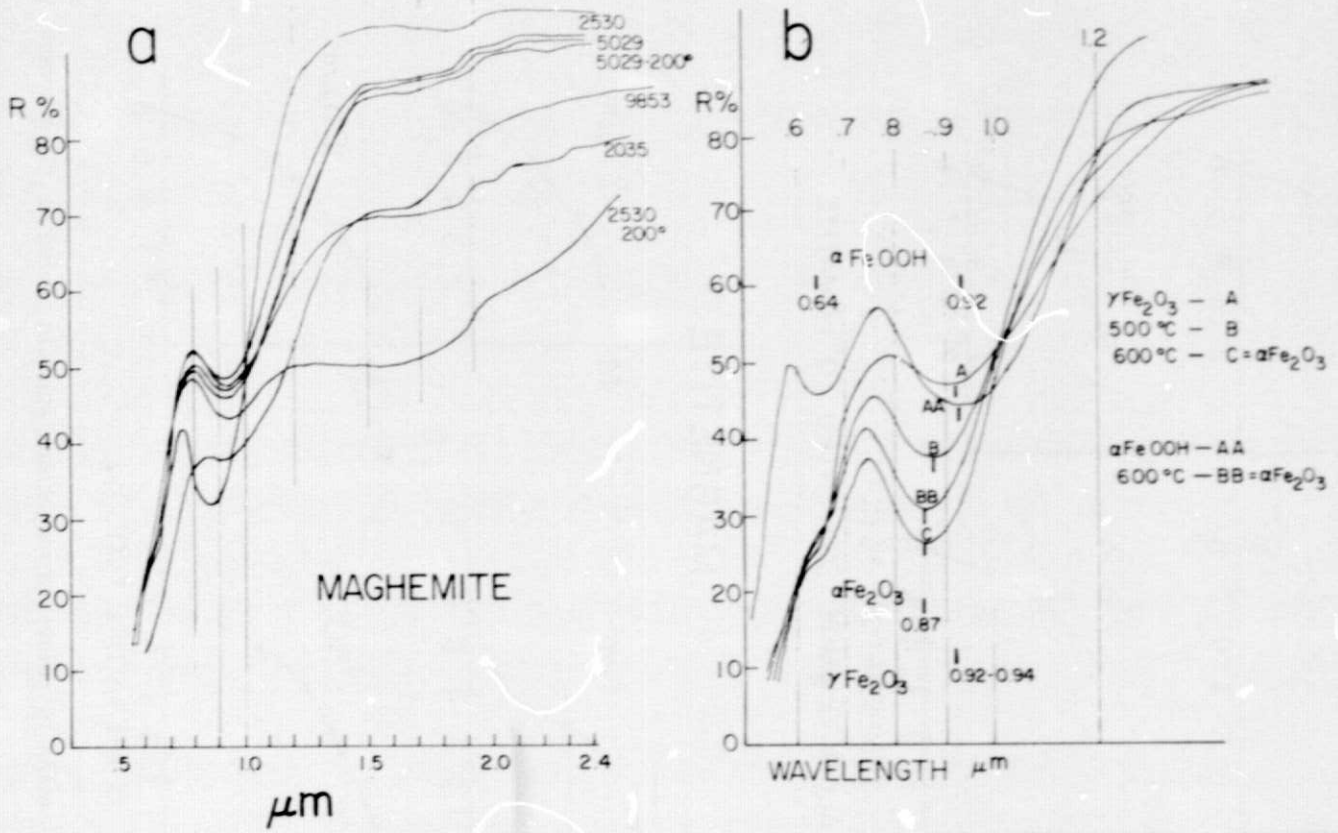

Figure 6. (a) Reflection spectra for maghemite specimens and for maghemites 5029 and 2035 after heating at 200°C for 1 hour in air. Also included is the spectrum for Fisher αFe_2O_3 powder.

(b) Reflection spectra for αFeOOH and γFe_2O_3 and the resultant αFe_2O_3 spectra obtained by heating at 600°C for 2 hours in air (FeOOH $\rightarrow \alpha Fe_2O_3$), and at 500°C and 600°C for 1 hour each ($\gamma Fe_2O_3 \rightarrow \alpha Fe_2O_3$). Fe^{3+} absorption features are identified.

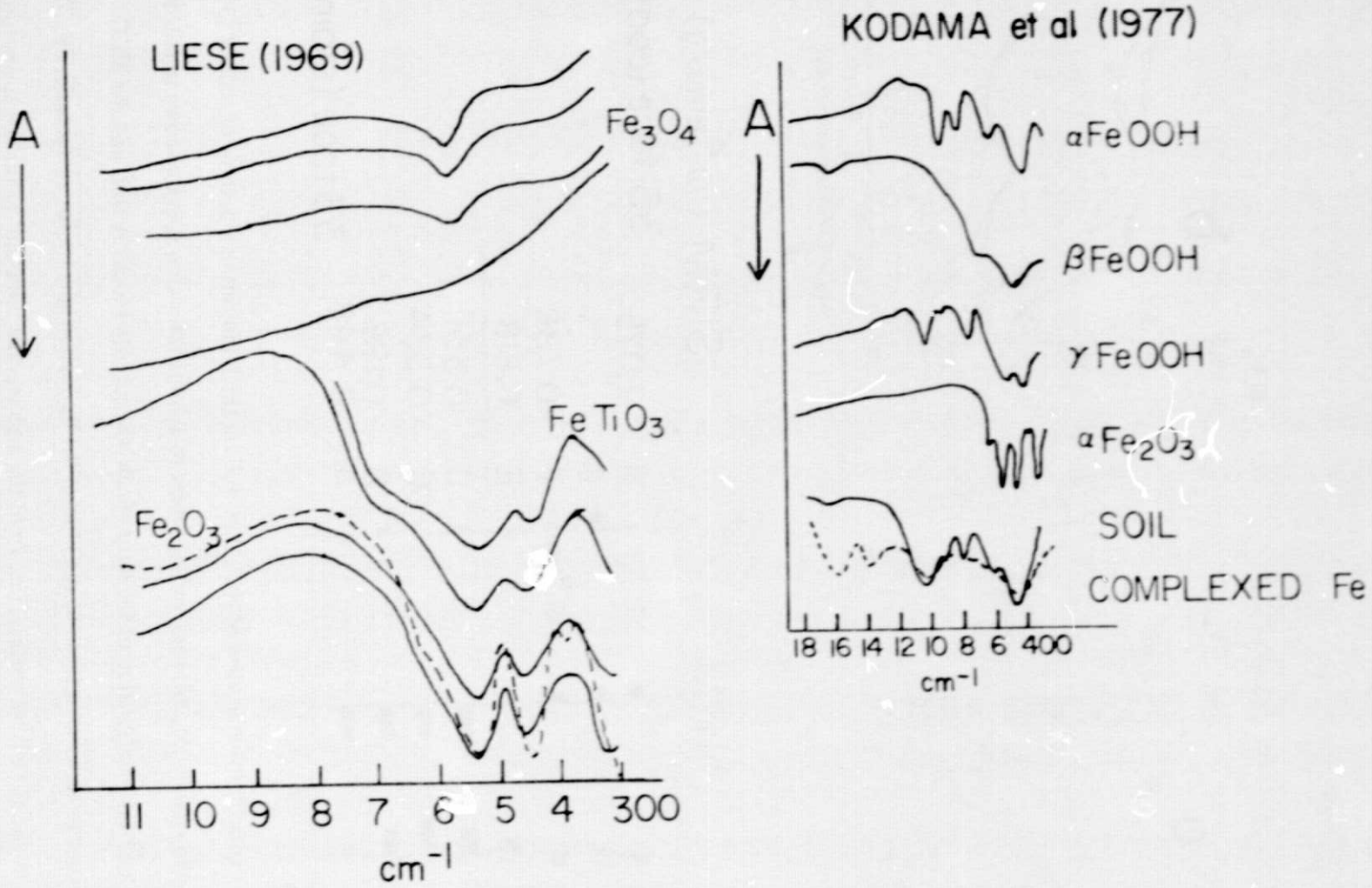

Figure 7. Absorption spectra taken from the literature (KBr pellet technique) for iron oxides.

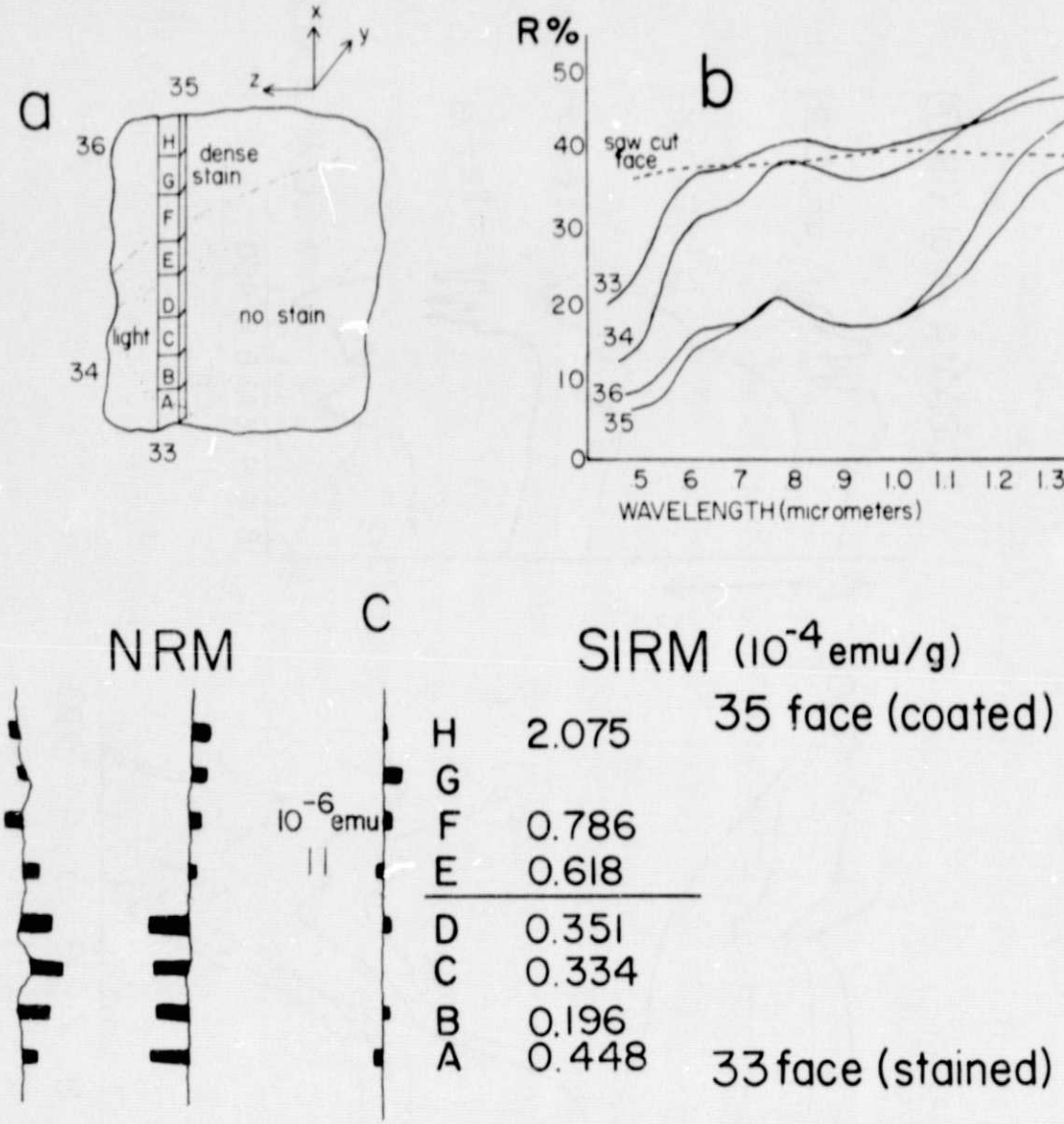

Figure 8. (a) Plan view of rock slice ~ 1 cm thick indicating locations of stained (33, 34) and coated (35, 36) rock surfaces used to acquire reflection spectra shown in (b), the approximate location of the strip which was cut into blocks A to H and the XYZ coordinate system fixed to the blocks. (b) Reflection spectra for surfaces 33, 34, 35 and 36 and for a fresh surface, i.e., from the area marked 'no stain' in (a). (c) Magnetometer record of NRM and SIRM for blocks A to H.

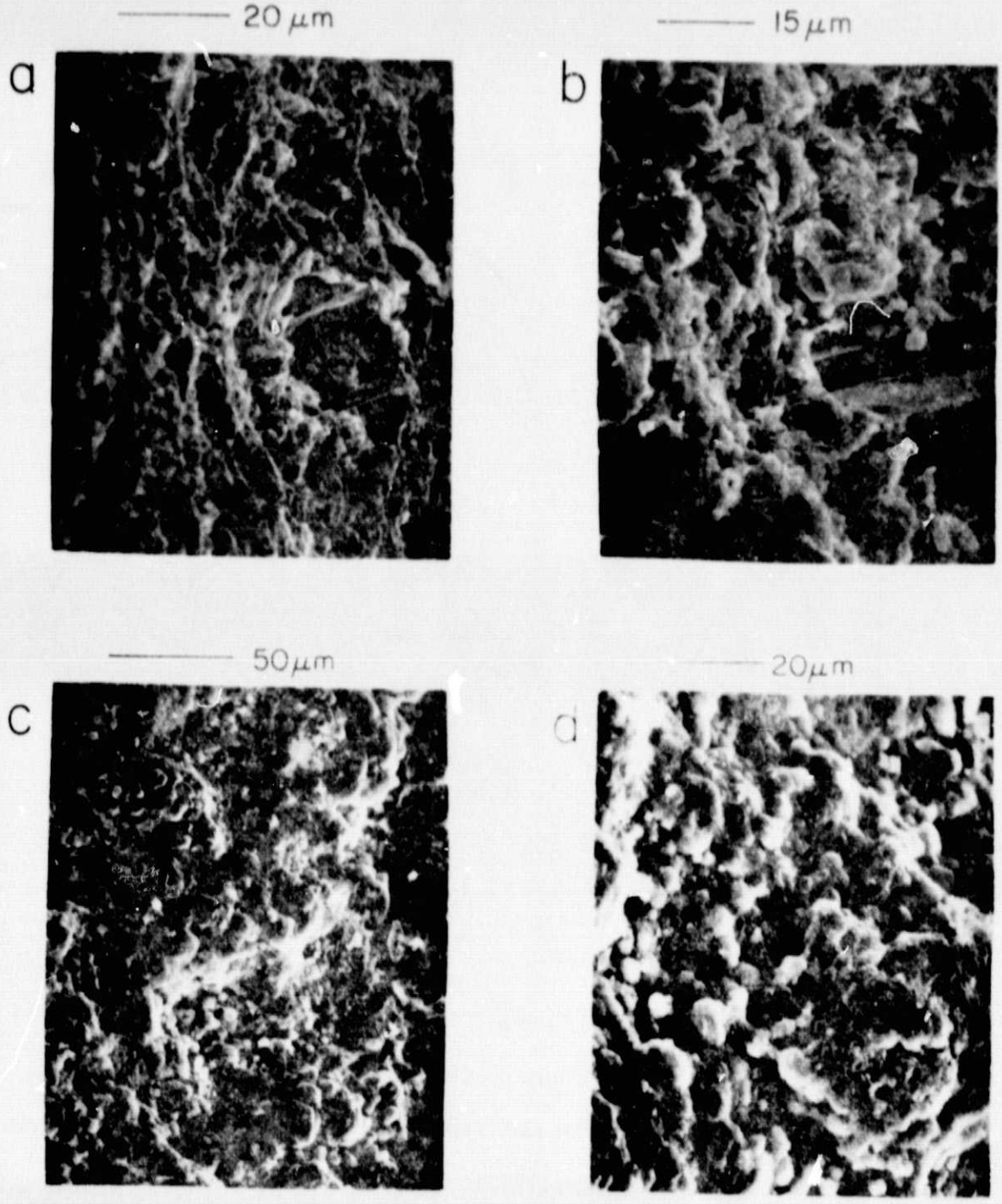

Figure 9. (a and b) Scanning electron micrographs of stained surface (33) illustrating crystalline surface and fine weathering products. (c and d) SEM of coated surface (36) which gives no indication of a crystal surface only a globular and continuous coating.

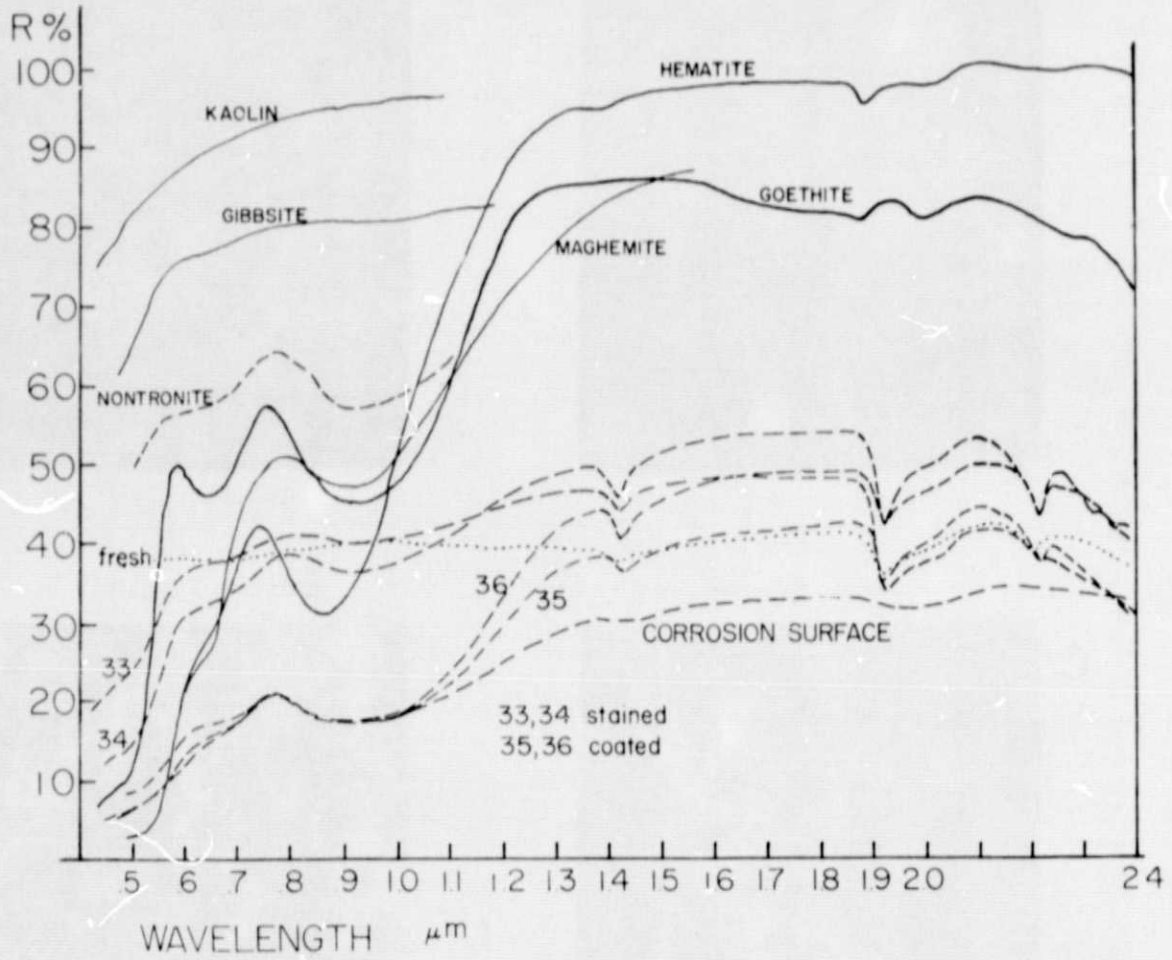

Figure 10. Reflection spectra (0.5 μm to 2.4 μm) for the same surfaces in Figure 8(b), a corrosion surface on a piece of Campo del Cielo iron meteorite (coated surface, αFe_2O_3, γFe_2O_3 and FeOOH. Included are partial spectra for Gibbsite, Kaolin and Nontronite (copied from Lindberg and Snyder (1972)).

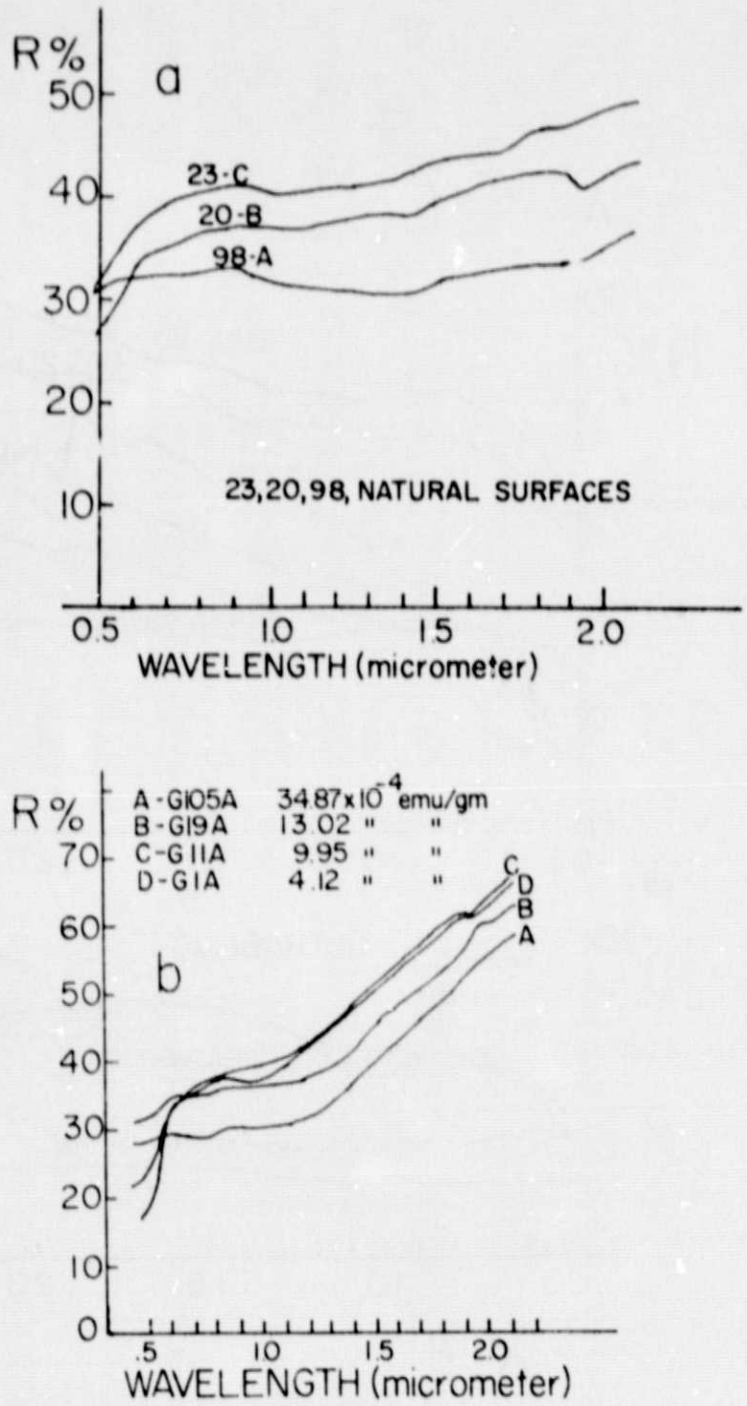

Figure 11. Reflection spectra from a fresh (98A) and two stained surfaces (23C, 20B) of Glen Alpine Stock granodiante.

(b) Reflection spectra from 200 mesh powders of Glen Alpine Stock granodiorites.

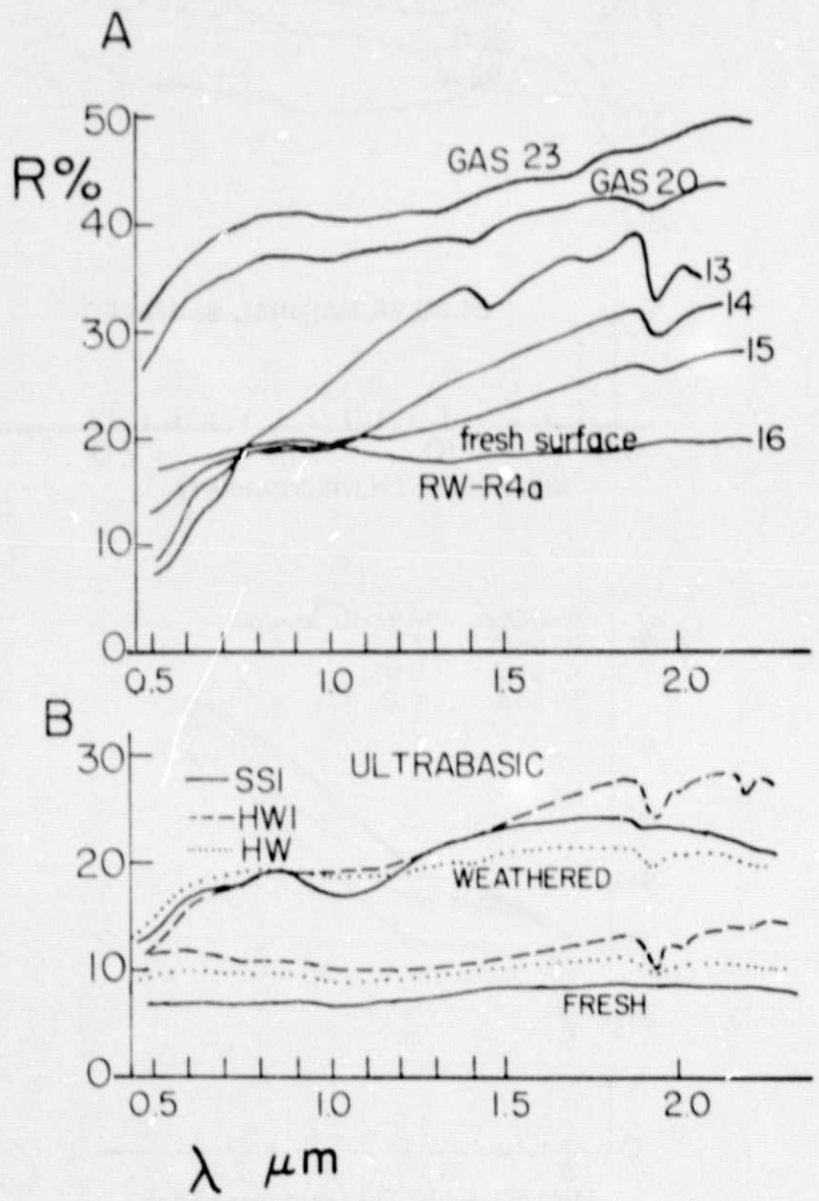

Figure 12. (a) Reflection spectra from granodiorite (stained surface GAS 23 and GAS 20) and diorite (fresh-16, stained-15, dense stain-14 and coated-13) surfaces. (b) reflection spectra from fresh and coated ultrabasics rocks.

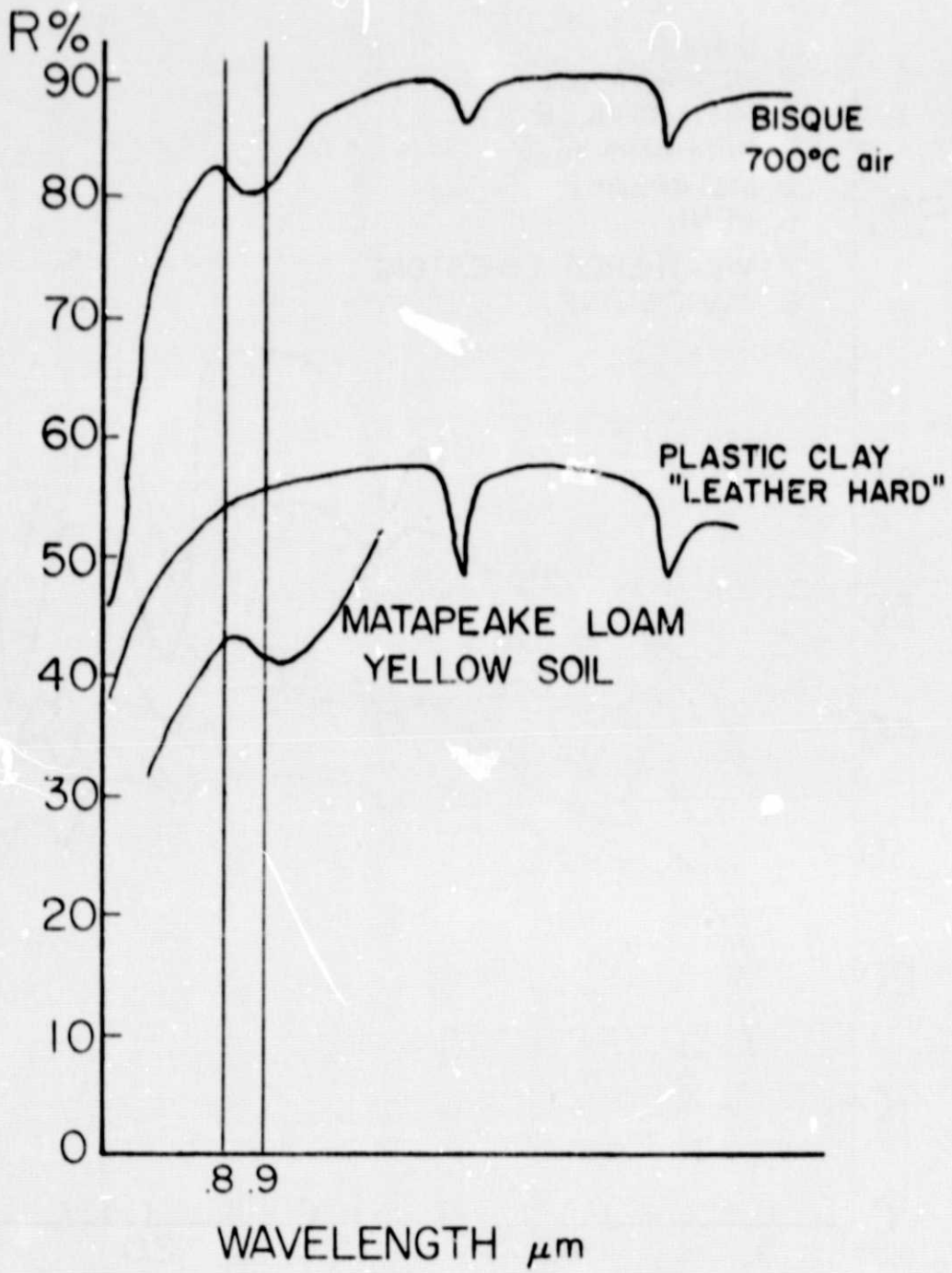

Figure 13. Reflection spectra for plastic potters clay dried to the 'leather hard' stage, and the same after firing at 700°C in flowing air (the Bisque firing). Also included is part of the reflection spectrum for Matapeake silt loam soil (a yellow soil).

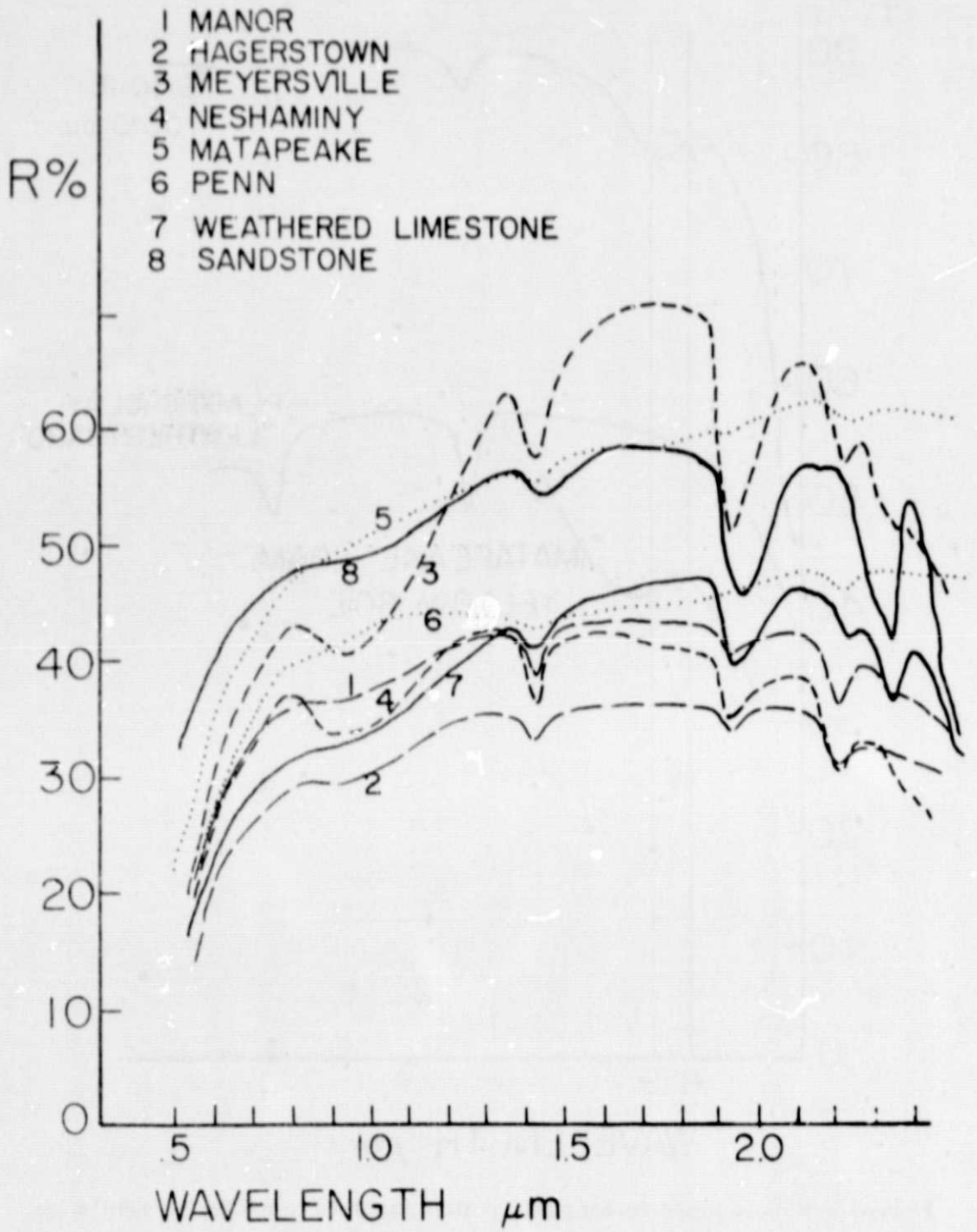

Figure 14. Reflection spectra for 6 Maryland silt loam soils, a 'white' sandstone surface and a clay covered surface of a limestone from West Virginia.

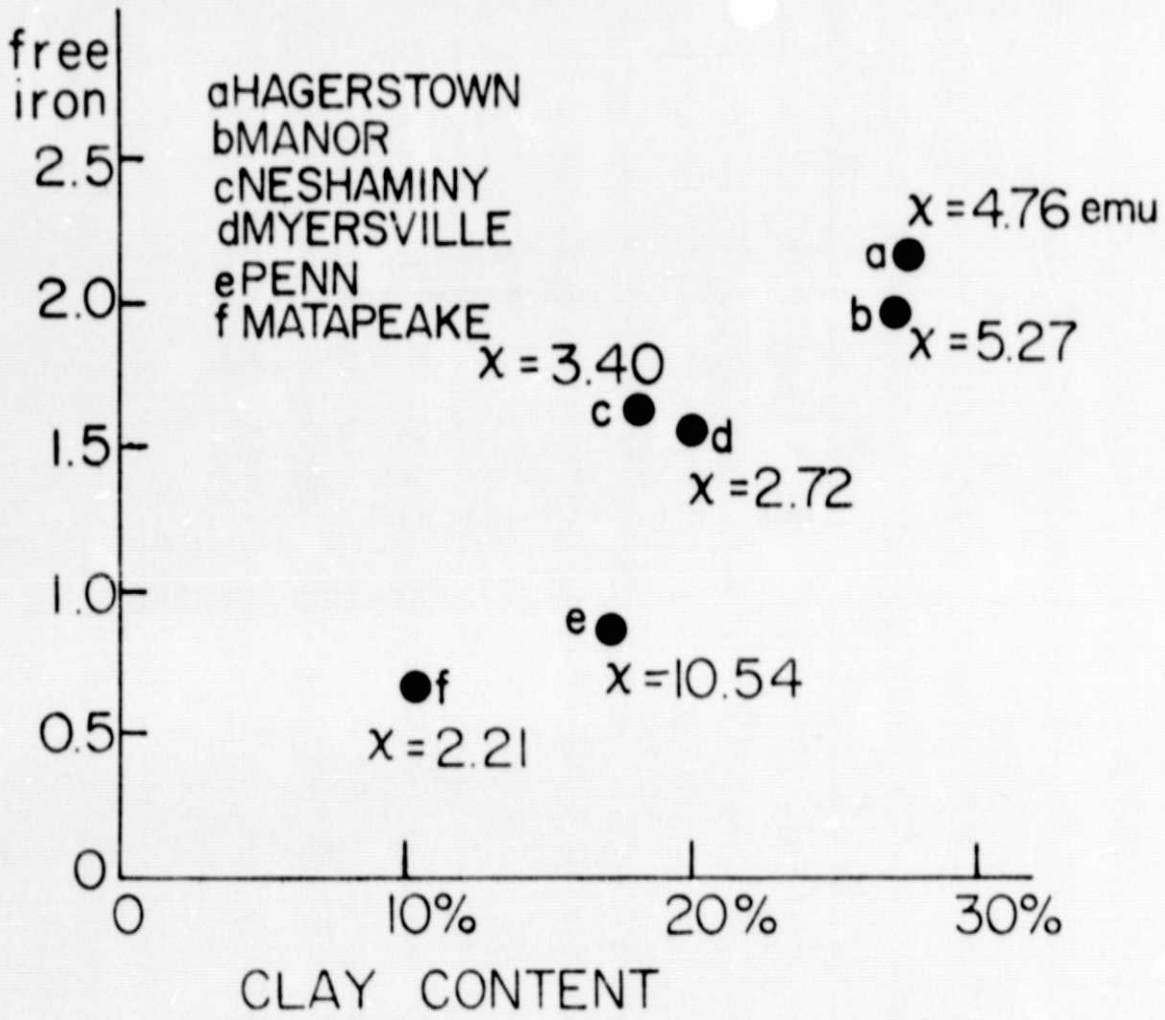

Figure 15. Plot of free iron content vs. clay content for the 6 Maryland soils. The magnetic susceptibility value for each of the soils is also indicated.

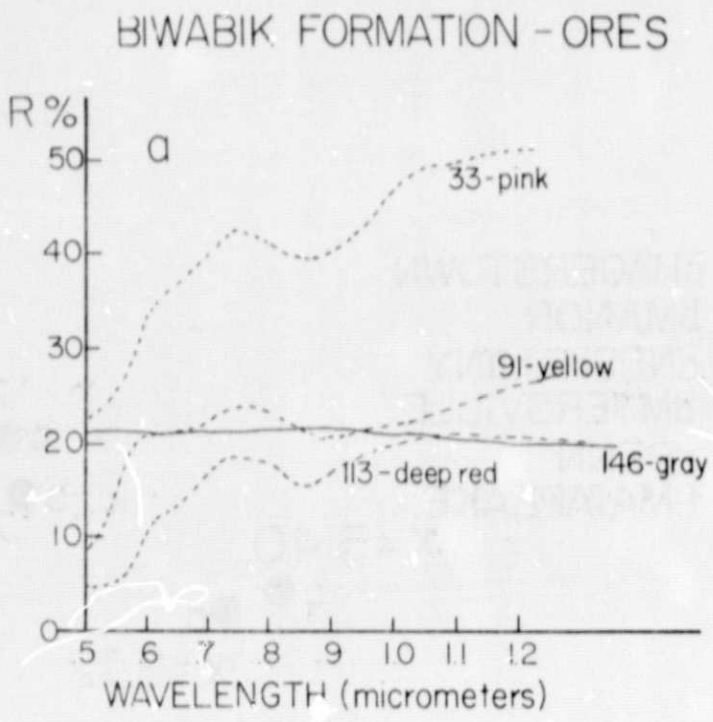

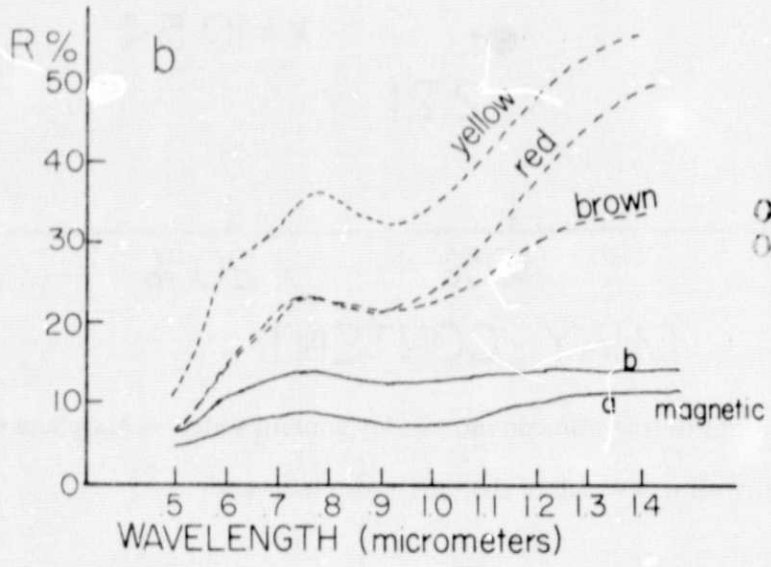

Figure 16. (a) Reflection spectra for 200-400 mesh powders from the Biwabik formation. (b) Reflection spectra for magnetic and non-magnetic meteoritic scale fractions separated initially by hand according to color and then subjected to magnetic separation to enhance color purity.

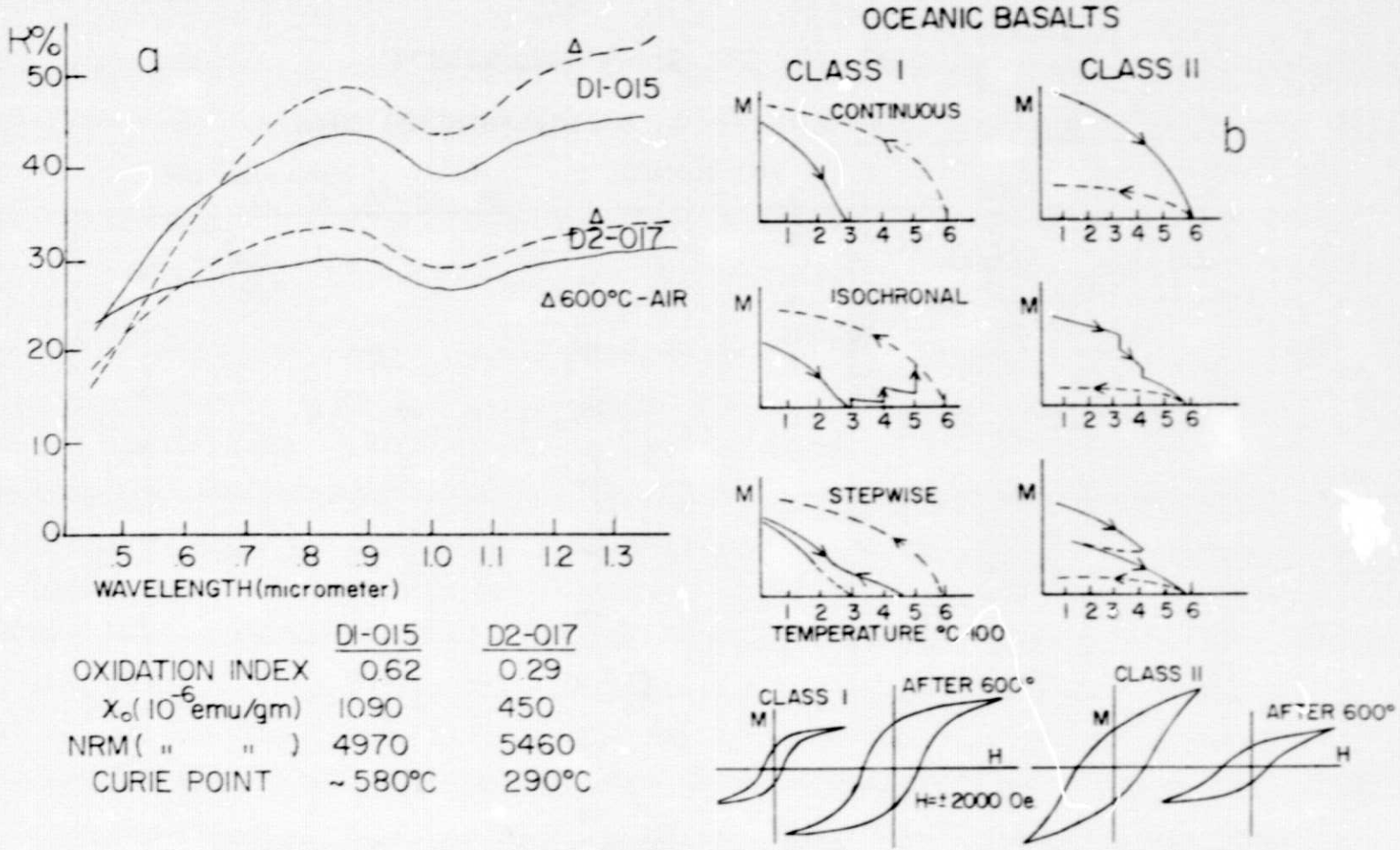

	D1-015	D2-017
OXIDATION INDEX	0.62	0.29
χ_o (10^{-6} emu/gm)	1090	450
NRM (" ")	4970	5460
CURIE POINT	~ 580°C	290°C

Figure 17. (a) Reflection spectra for Class I (D2017) and Class II (D1015) basaltic rocks before and after heating.

(b) Summary of magnetic characteristics of Class I and Class II basaltic rocks (after Wasilewski, 1968).

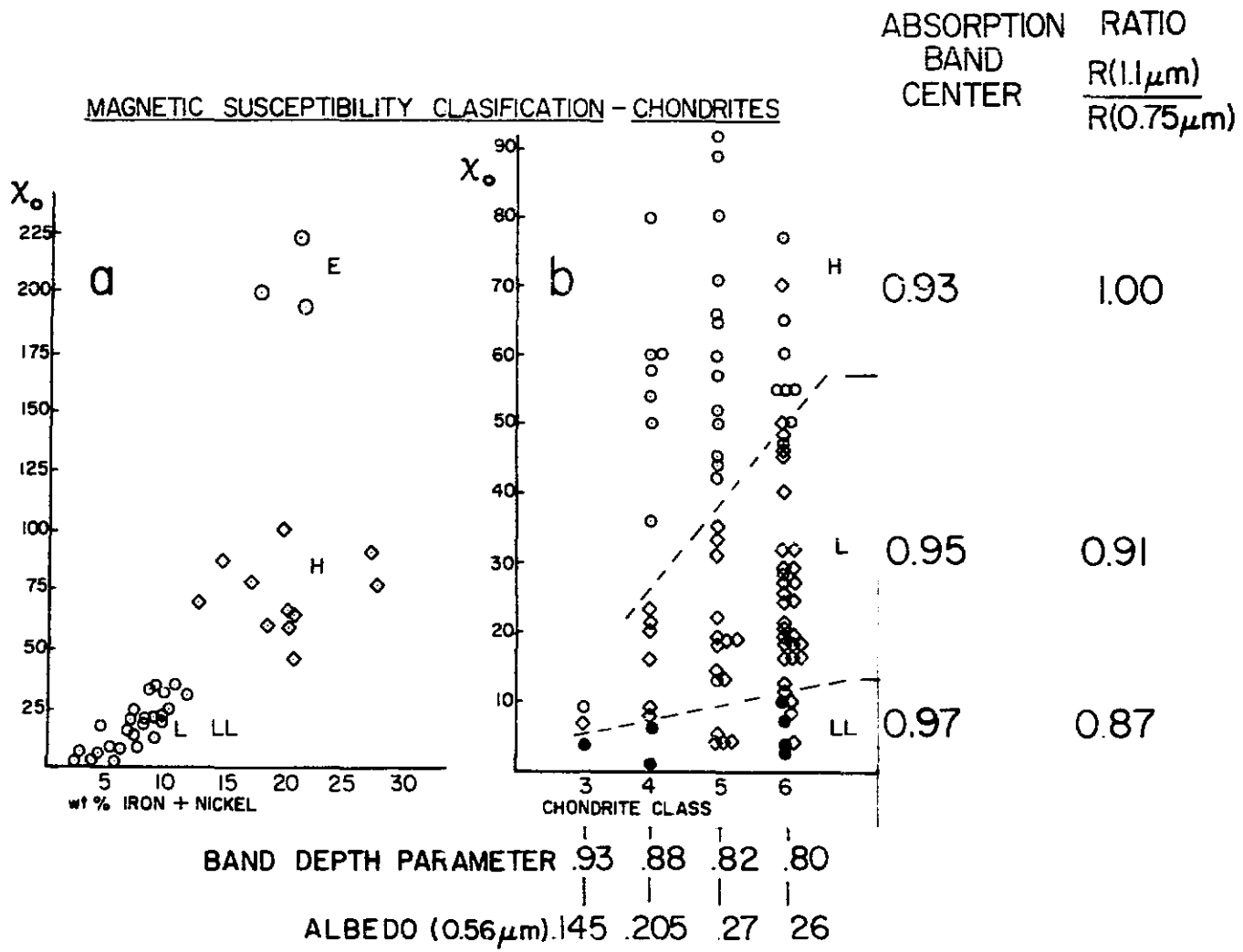

Figure 18. Plot of initial susceptibility (χ_o) vs wt % Fe + Ni and vs chondrite petrologic class. Included in the χ_o vs class diagram are reflection curve parameters from Chapman and Salisbury (1973).